



Published by Fusion Energy Division, Oak Ridge National Laboratory  
Building CR 5600 P.O. Box 2008 Oak Ridge, TN 37831-6169, USA

Editor: James A. Rome

Issue 135

February 2012

E-Mail: jamesrome@gmail.com Phone (865) 482-5643

On the Web at <http://www.ornl.gov/sci/fed/stelnews>

## Spatiotemporal structure of the turbulence-flow interaction at the L-H transition in TJ-II

### Introduction

The H-mode confinement regime has been extensively studied since its discovery in ASDEX [1]; however, the physical mechanism triggering the H-mode has still not been clearly identified. Bifurcation theory models, based on the coupling between turbulence and flows, describe the L-H transition as passing through an intermediate, oscillatory transient stage with a characteristic predator-prey relationship between turbulence and zonal flows [2].

This intermediate oscillatory transient stage has been seen in the L-H transition experiments in TJ-II [3] as well as in other devices. In these experiments, as in the predator-prey theory model [2], only the temporal dynamics of the turbulence-flow interaction is studied.

However, as recently pointed out [4], the spatial evolution should also be taken into account as a necessary step in developing a model for the L-H transition model.

The present work, a summary of the results recently reported in Ref. [5], addresses this fundamental issue from an experimental point of view for the first time.

### Experimental Results

The experiments have been carried out in the TJ-II stellarator. A two-channel Doppler reflectometer is used to measure the radial electric field  $E_r$  and density fluctuations,  $\tilde{n}_e$  at two radial positions simultaneously with good spatial and temporal resolution [6]. As reported in Ref. [3], close to the L-H transition threshold pronounced oscillations in both  $E_r$  and  $\tilde{n}_e$  are measured at the plasma edge, just inside the  $E_r$  shear position. Depending on the NBI heating power and magnetic configuration, the oscillations can endure throughout the NBI heating phase of the discharge. Simultaneous with the onset of the oscillations, there is a drop in the  $H_\alpha$  signals and an increase in diamagnetic energy,  $W_{\text{dia}}$  and  $n_e$ . The oscillations appear as changes in

the intensity and frequency of the Doppler reflectometry spectra and show a predator-prey relationship between turbulence and flows, with the flow—the predator—following the turbulence—the prey—with a phase delay of  $90^\circ$  in a limit-cycle way [3].

The radial profile of  $E_r$ , shown in Fig. 1, changes from rather flat in L-mode to sheared during the oscillating phase. The  $E_r$  oscillation amplitude is about 1 kV/m close to the  $E_r$  shear and increases gradually as inner radial positions are probed. As a consequence, the  $E_r$  well of about 10 kV/m measured at the maximum of the oscillations shrinks in each limit-cycle and an inner shear layer develops at  $\rho \approx 0.75$  (see blue profile in Fig. 1).

### In this issue . . .

#### Spatiotemporal structure of the turbulence-flow interaction at the L-H transition in TJ-II

The spatiotemporal structure of the turbulence-flow interaction has been measured at the L-H transition in TJ-II plasmas. The temporal dynamics of the interaction displays an oscillatory behavior with a characteristic predator-prey relationship. The spatiotemporal evolution of this oscillation pattern shows both radial outward and inward propagation velocities of the turbulence-flow front. The results indicate that the edge shear flow linked to the L-H transition can behave either as a slowing-down, damping mechanism of outward propagating turbulent-flow oscillating structures, or as a source of inward propagating turbulence-flow events. . . . . 1

#### W7-X status report

The five torus modules are in place, and two modules have their ports installed. Interior component installation and connections between each torus module are under way. . . . . 4

All opinions expressed herein are those of the authors and should not be reproduced, quoted in publications, or used as a reference without the author's consent.

Oak Ridge National Laboratory is managed by UT-Battelle, LLC, for the U.S. Department of Energy.

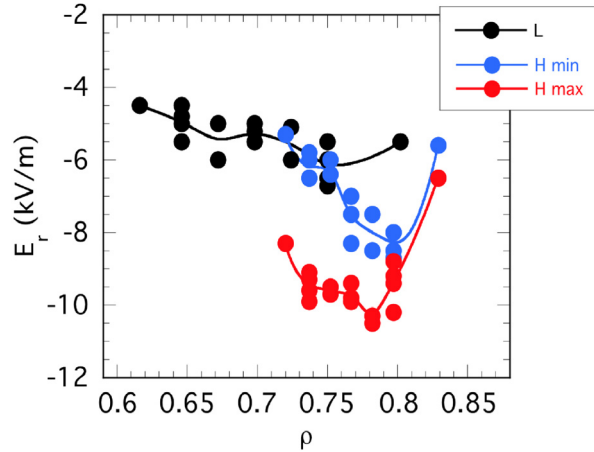


**Fig. 1.**  $E_r$  profiles in L-mode (black) and during the intermediate oscillatory phase:  $E_r$  maxima (red) and minima (blue) measured at  $n_e \sim 2.0\text{--}2.5 \times 10^{19} \text{ m}^{-3}$ .

The measurement of the radial propagation characteristics of the oscillation pattern allows extension of the previous temporal characterization to a spatiotemporal one. An example is shown in Fig. 2, which displays the time evolution of both (a),  $\text{rms}(\tilde{n}_e)$  and (b)  $E_r$  measured simultaneously at  $\rho = 0.8$  and  $\rho = 0.75$ . In addition, the time evolution of  $E_r$  shear is shown in Fig. 2(c).

The relation between  $E_r$  shear and  $\text{rms}(\tilde{n}_e)$  showing a limit-cycle behavior is shown in Fig. 2(d). Pronounced changes in  $E_r$  shear appear linked to the oscillations in  $\text{rms}(\tilde{n}_e)$ . A delay between the two channels can be seen, indicating a radial propagation from the inner to the outer channel. This outward propagation is found at line densities between  $2\text{--}2.5 \times 10^{19} \text{ m}^{-3}$ . At densities above  $3 \times 10^{19} \text{ m}^{-3}$ , the propagation direction in some cases reverses after a short time without oscillations. Analysis of the delay yields propagation velocities within the range  $50\text{--}200 \text{ m/s}$  with a radial trend as shown in Fig. 3. In this figure the vertical bars represent the error in the estimation of the propagation velocity and the horizontal ones represent the radial separation between the two radial channels. The radial propagation velocity decreases as the turbulence-flow front approaches the  $E_r$  shear position. The inward propagation velocity has similar values but no clear radial dependence can be inferred. The extreme values of the  $E_r$  oscillations are comparable in both cases but the time evolution shows differences. As the turbulence-flow front propagates outward, the increase in the turbulence level produces an increase in the inner shear; however, a turbulence-flow front propagating inward produces an increase in the outer shear.

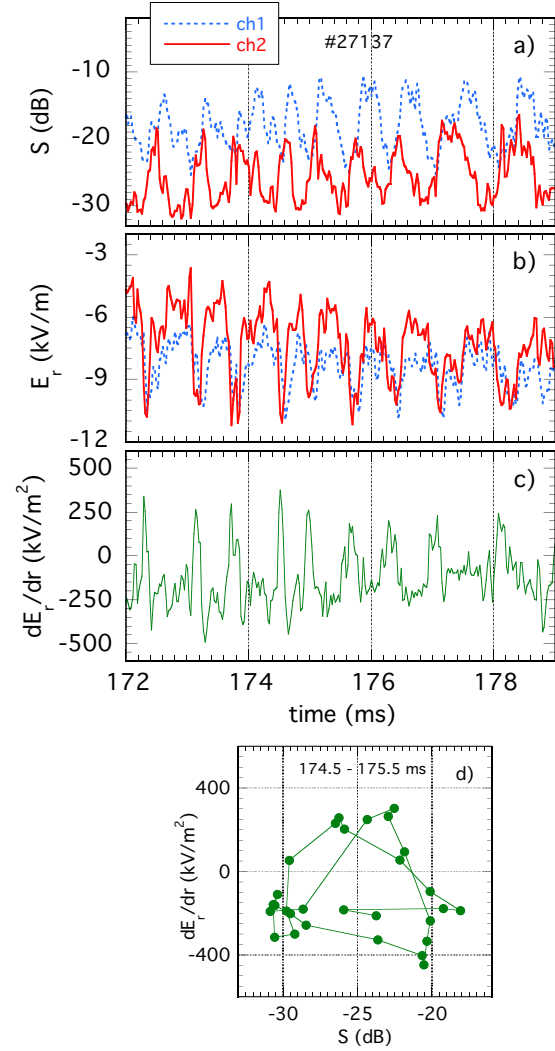


**Fig. 2.** The time evolution of (a)  $\text{rms}(\tilde{n}_e)$  and (b)  $E_r$  measured at  $\rho = 0.8$  (blue) and  $\rho = 0.75$  (red). (c) The time evolution of  $E_r$  shear and (d) relation between  $E_r$  shear and  $\text{rms}(\tilde{n}_e)$ .

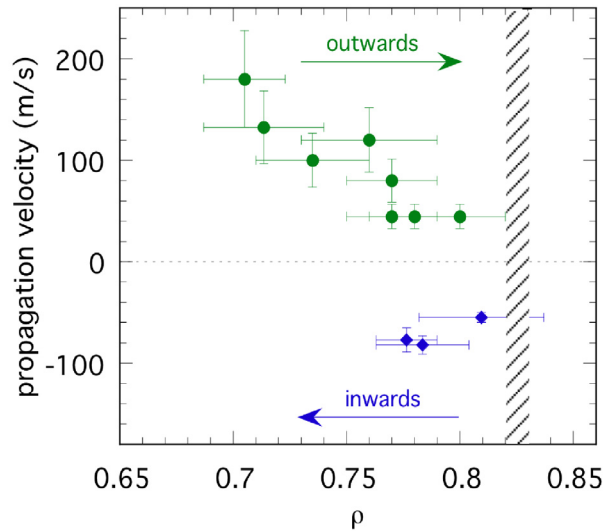


**Fig. 3.** Radial propagation velocity of the turbulence-flow front. The striped area indicates the  $E_r$ -shear position.

### Summary and discussion

The spatiotemporal evolution of the oscillation pattern could be linked to the radial spreading of plasma turbulence from the plasma core to the edge barrier. Previous experiments performed in TJ-II have shown signatures of radial spreading of the turbulence as the plasma approaches the H-L back transition condition [7]. Similarly, in the present experiments, as the turbulence propagates towards the barrier, the associated turbulence-driven flow generates the inner shear layer, which in turn regulates the turbulence level. The present observation could be also understood in terms of turbulent bursts propagating toward the plasma edge. These turbulent bursts could be generated in the plasma interior by instabilities linked, for instance, to the magnetic topology. To explain the present experimental observations, each turbulent burst should be accompanied on its way to the plasma edge by a sheared-flow layer. The deceleration in the oscillation-pattern propagation as it approaches the edge shear layer together with its absence at outer radial positions suggest an absorption process at the  $E_r$  shear layer. In this process, the turbulence-flow events generate a dual shear layer and thus enhance the formation of the  $E_r$  well.

A reversal in the front propagation velocity is observed in some cases at the final stage of the discharge after a quiet period without oscillations. In those cases the oscillation pattern arises at the outer shear layer position and propagates towards the plasma interior.

The present experimental results indicate that the edge shear flow linked to the L-H transition can behave either as a slowing-down, damping mechanism of outward propagating turbulent-flow oscillating structures, or as a source of inward propagating turbulence-flow events.

The reported results show the need to approach L-H transition studies within a 1-D spatiotemporal framework.

T. Estrada and the TJ-II team

E-mail: [teresa.estrada@ciemat.es](mailto:teresa.estrada@ciemat.es)

Phone: 34 91 346 0845

Laboratorio Nacional de Fusión. As. Euratom-CIEMAT, 28040 Madrid, Spain

### References

- [1] F. Wagner et al., Phys. Rev. Lett. **49**, 1408 (1982).
- [2] E.-J. Kim and P.H. Diamond. Phys. Plasmas **10**, 1698 (2003).
- [3] T. Estrada et al., Europhys. Lett. **92**, 35001 (2010).
- [4] P.H. Diamond et al., Plasma Phys. Control. Fusion **53**, 124001 (2011).
- [5] T. Estrada et al., Phys. Rev. Lett. **107**, 245004 (2011).
- [6] T. Happel et al., Rev. Sci. Instrum. **80**, 073502 (2009).
- [7] T. Estrada et al., Nucl. Fusion **51**, 032001 (2011).

## W7-X status report

### W7-X torus completed

On 16 November 2011, the last of the five field-period modules that comprise the Wendelstein 7-X (W7-X) stellarator in Greifswald, Germany, was placed on its foundation with millimeter precision, as shown in Fig. 1. The entire procedure required only 3 hours although the assembly team had expected a considerably longer process because for the first time, it was necessary to avoid collision at both ends of the module. As little as 8 mm of clearance was available—often at several points simultaneously—in maneuvering the 120 tonne module into position.

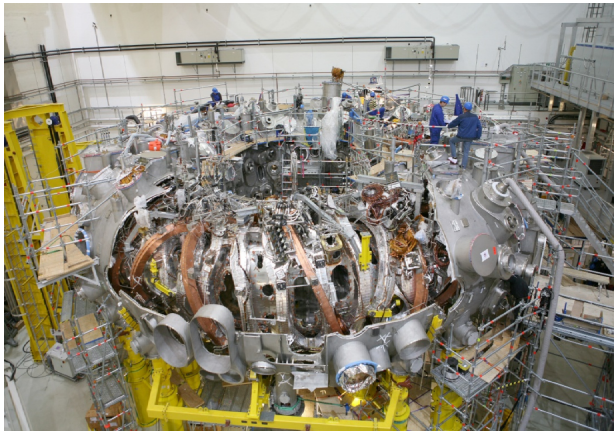


**Fig. 1.** Wendelstein 7-X on 16 November 2011.

In the coming months, each module will be connected to its two neighbors. The separate cryopiping, instrumentation, and bus systems of the individual modules will then be joined using superconducting joints where necessary. The sections of the central support ring will be bolted

together, the thermal insulation joined at the seams, and the plasma and external vessels joined by welding.

At the beginning of 2012, assembly of the in-vessel components will commence by cladding the plasma vessel with stainless steel cooling panels. Regions that will be subjected to high thermal loads must be protected with carbon tiles.

### Ports provide access to the plasma

Before assembly of the numerous in-vessel components can begin, however, it is necessary to install the ports that will provide the links between the interior and exterior of the plasma vessel.

There is a total of 254 vacuum-tight ports, some as long as 3 m. Roughly half of the ports are devoted to diagnostic purposes; the remainder provide access for plasma heating systems and for the vacuum pumps. Also accommodated by the ports is the water-filled piping, which is used for cooling the vacuum vessel. See Fig. 2.

The shapes of the port openings vary from circular with a diameter of 150 mm to approximately rectangular with dimensions of  $1000 \times 4000 \text{ mm}^2$ . The largest ports are reserved for microwave and neutral-beam heating systems and to provide physical access to the torus for maintenance.

Placement of the ports is done from outside the torus. This involves insertion through the opening in the external vessel and maneuvering through the cryo chamber to the target position on the plasma vessel, after which both ends are welded into place.

To accommodate movement of the plasma vessel during experimental operation of W7-X, connection of the ports to the external vessel makes use of bellows. Because the ports must pass through the extreme cold of the cryo chamber, it is mandatory that they be carefully insulated.

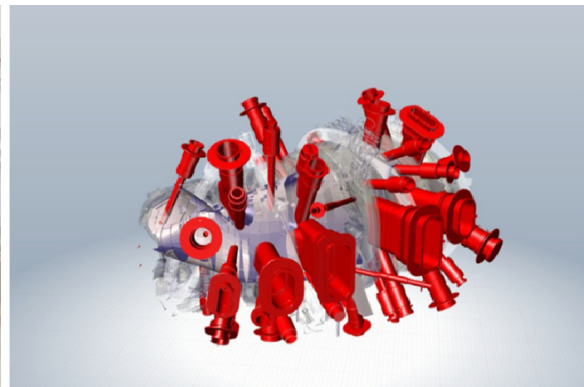


**Fig. 2.** Real and virtual perspectives: the photo on the left shows a module without ports in the experimental hall. On the right is a CAD view of the same region (with external vessel removed) with the ports highlighted in red.

In accordance with the project timetable, port assembly has been completed for three of the five modules. This was achieved in spite of the technical challenges faced during the process. Indeed, ports weighing as much as a tonne have been maneuvered and welded in place with the require millimeter precision.

Determination of correct lengths and the complicated curves along which the ports must be cut to shape was also technically demanding. The initial approach, which involved provisional placement of each port and subsequent cutting to achieve a satisfactory fit, has now been replaced with a three-dimensional (3-D) construction technique (Fig. 3) which accounts not only for the plasma vessel shape and the port orientation, but also distortion that can be expected during the welding process. Once the port has been cut to the correct shape it must be thermally insulated. To prevent subsequent collisions in construction and in the operation of W7-X, the insulation must also be applied with millimeter accuracy.



**Fig. 3.** For the accurate placement of the ports it was necessary to develop a carriage system encompassing 5 degrees of freedom at heights of up to 12 m above the floor of the experimental hall.

### **Zero tolerance—engineering pushed to its limits**

A handful of ports pose special challenges as they require accuracy at the level of technical feasibility. Although in most cases tolerances of a few millimeters are allowed, these special ports have tolerances that are essentially zero. The reasons for this include maximization of the port

cross sections and the necessity of avoiding collisions with other components.

An example is the port for neutral particle heating. Reduction of the port cross section by as little as 1 mm would significantly increase the number of fast particles that never reach the plasma and instead deposit their energy onto the port. An increase in port dimensions is impossible in this case due to the surrounding components, including the magnetic field coils. To improve such situations an iterative design and test procedure is used in which the orientation and welding properties of prototype ports are investigated with current results incorporated into each subsequent design.

This approach requires teamwork of the highest level as it represents an interplay of scientific calculations, modern CAD modeling, accurate 3-D measurements, cutting-edge engineering and a fine human touch.

Prof. Dr. Robert Wolf and Dr. Andreas Dinklage for the W7-X Team

E-mail: [w7xnewsletter@ipp.mpg.de](mailto:w7xnewsletter@ipp.mpg.de)

Max-Planck-Institut für Plasmaphysik

Association Euratom – IPP

Wendelsteinstraße 1

Germany - 17491 Greifswald